A CFD Investigation of Piping System Design for a Tank Cleaning Machine

Didi Widya Utama
Mechanical Engineering Department, Universitas Tarumanagara, Jakarta, Indonesia
didiu@ft.untar.ac.id

Choon Kit Chan
Department of Mechanical Engineering, INTI International University, Nilai, Malaysia
choonkit.chan@newinti.edu.my (corresponding author)

Ravi Hardian
Mechanical Engineering Department, Universitas Tarumanagara, Jakarta, Indonesia
ravi.515200004@stu.untar.ac.id

Agustinus Purna Irawan
Mechanical Engineering Department, Universitas Tarumanagara, Jakarta, Indonesia
agustinus@untar.ac.id

Jeyagopi Raman
Department of Mechanical Engineering, INTI International University, Nilai, Malaysia
jeyag.raman@newinti.edu.my

Received: 23 July 2025 | Revised: 8 September 2025 | Accepted: 18 September 2025

 DOI: https://doi.org/10.48084/etasr.13595

ABSTRACT

In industries that focus on food, beverage, and pharmaceutical manufacturing, the hygiene of production equipment is mandatory and must always be maintained. Cleaning equipment for such an industry is essential and needs to be designed as required. This study addresses the need for uniform pressure distribution within the nozzle to ensure optimal operation. Equal spray direction, pressure, and distribution are necessary so that the water impact on the tank surface is uniform, thereby maximizing the cleaning effectiveness. This research develops a cleaning system for industrial material storage tanks. The proposed system utilizes pressurized water spraying to remove dust, particles, and unwanted substances that may compromise production quality. The experimental program compares eight piping ring configurations for tank cleaning equipment, where the ring has one inlet and eight outlets; each outlet is attached to a flat fan nozzle. To investigate the fluid flow in the designs, Computational Fluid Dynamics (CFD) simulation was used to examine fluid flow phenomena in the tank cleaning ring and identify the minor pressure drop at the nozzle. After selecting the best design, calculations were carried out to determine the pump's specifications used in the tank cleaning machine installation.

Keywords-cleaning machine; piping system; fluid vortex; Computational Fluid Dynamics (CFD); head loss; process innovation

I. INTRODUCTION

The pharmaceutical, food, and beverage industries require a tank-cleaning machine to clean and sterilize production objects, equipment, materials, and tools effectively [1]. The hydraulic efficiency of disinfection systems is crucial in the design and operation of cleaning equipment, particularly in chlorine contact tanks, to avoid the formation of potential carcinogenic products during the disinfection process [2]. After cleaning, wastewater can be reused to support more efficient water usage [3]. Furthermore, optimizing water systems with the consideration of pressure drop and pumping is a crucial aspect to explore for the development of effective tank-cleaning machines [4].

The optimization of the piping system to minimize pressure deviation is a critical aspect in maintaining a minimal pressure drop. Previous studies have addressed the piping cost in the optimization of water networks, yet design issues associated

with pressure drop and pumping have not been thoroughly explored [4]. The influence of pressure drop in the piping system on the spraying performance of flat nozzles is a critical consideration in various applications. As the backpressure increases, the spray width downstream also increases, indicating a direct correlation between the pressure drop and the characteristics of the spray [5]. Additionally, the investigation of pressure drops in horizontal pipes with different diameters has provided insights into the relationship between the pipe dimensions and pressure drops, which is essential in understanding the impact of the piping configurations on spraying performance [6]. CFD analysis has been widely utilized to analyze the vortex fluid flow inside pipes and optimize the piping system configurations. Research has explored the application of CFD simulations to analyze the cavitation flows inside injector nozzles, providing insights into the fluid dynamics and spray characteristics [5, 7].

This study investigates the design of tank-cleaning machine installations. The primary focus lies in selecting the optimal configuration design for a tank cleaning ring by elaborating computational methods. This helps streamline the fluid flow more efficiently, ensuring fluid pressure and that the speed aligns with the nozzle specifications. CFD simulations are utilized to model the fluid flow across eight-piping ring models, focusing on examining the pressure distribution and velocity at each outlet nozzle. Following the CFD simulations, theoretical calculations were conducted to determine the specifications for component selection [7, 8].

II. SYSTEM DESIGN

The piping installation for the tank cleaning machine is designed with carefully selected components that facilitate an efficient fluid flow. A schematic diagram of the piping installation is illustrated in Figure 1. Both water tanks are supplied to a centrifugal pump to build water pressure within the tank wall cleaning system. This type of pump employs centrifugal force to move fluids and is particularly effective for enhancing the fluid pressure in the installation [2]. Additionally, the system includes a valve that regulates the direction of the fluid flow. A solenoid valve [9], which can be automatically controlled to open or close, is employed for this purpose [10].

This study emphasizes the selection of readily available piping components to support efficient and cost-effective manufacturing processes. Subsequently, CFD analyses are conducted to assess the pressure drop within the system and determine the optimal configuration for the piping cleaning system. Additionally, a tank cleaning system designed for the external surfaces of the tanks is presented in Figure 2.

A. Geometry Model

The piping geometry model includes eight distinct configurations of piping rings. The CAD geometry was developed using Autodesk Fusion 360 software. Each configuration features one inlet and eight outlets, all designed with a 1-inch pipe size. Each outlet incorporates a fan flat nozzle, as depicted in Figure 3, which is particularly effective for spraying fluids in cleaning and painting applications due to its fan-shaped spray pattern. The inscribed diameter of the piping ring measures 1200 mm, as portrayed in Figure 4.

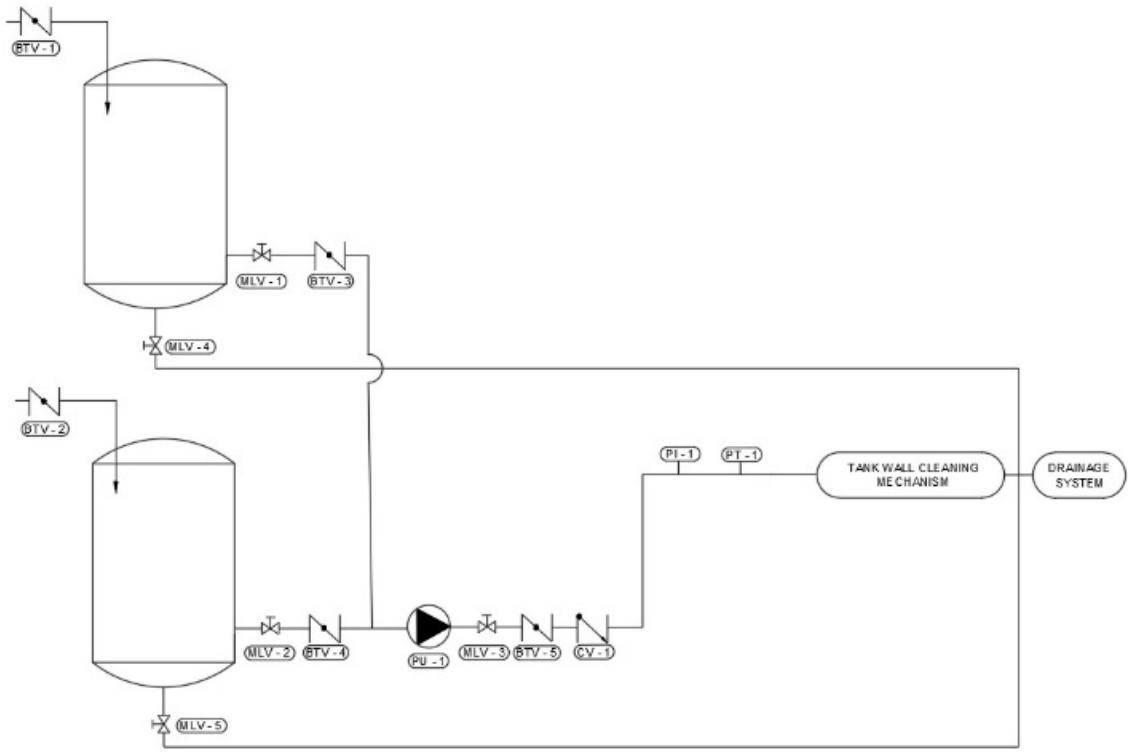

Fig. 1. A schematic diagram of the piping installation.

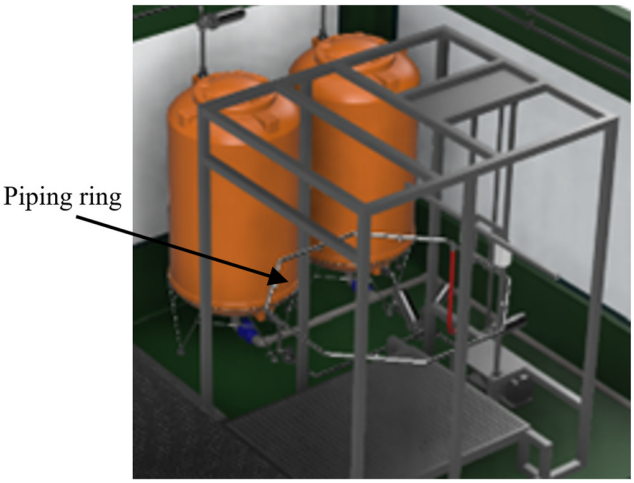

Fig. 2. Tank cleaning machine with the piping ring configuration at the center.

To optimize the fluid flow within the ring, two types of Tees are employed: the regular Tee, which has three junctions, and the Tee Y junction type, also shown in Figure 3.

Fig. 3. Geometry of regular Tee, Tee Y, and Flat Fan Nozzle (left to right).

The piping ring configuration has been developed with eight variations aimed at identifying the most optimized designs. Figure 5 illustrates these configurations, categorized into two main types: hexagonal and circular, along with their respective fluid flow directions. Each category encompasses different designs that include closed loops with Tee connectors, open loops with Tee connectors, split open loops featuring Tee Y-types, and closed loops with Tee Y-types.

The closed-loop system has one inlet that splits into two branches using a Tee, allowing fluid to flow to both the left and right rings in a continuous loop. In contrast, the open-loop system features a single inlet, where fluid flows in just one direction through a single channel.

B. Meshing and Boundary Conditions

Meshing refers to the discretization of a computational domain into a finite number of elements. The selection of mesh type and element size in CFD simulations plays a critical role in determining both the accuracy and convergence of the numerical results. The mesh configurations employed in the present study are summarized in Table I. Furthermore, a mesh independence study was conducted to identify the optimal mesh settings that ensure reliable results while minimizing the computational cost.

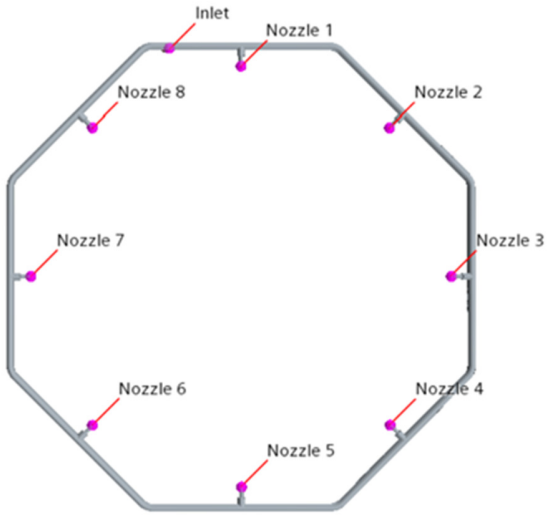

Fig. 4. Piping ring with inlet and nozzle configuration.

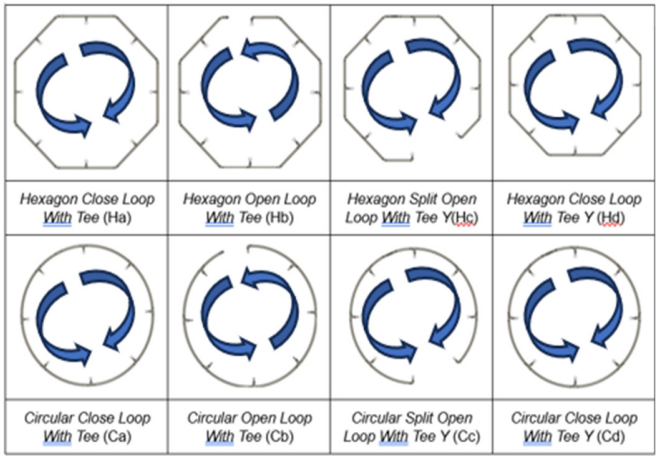

Fig. 5. Piping ring design configurations with inlet and nozzle.

TABLE I. MESH CONFIGURATIONS

Nodes	Values
Mesh type	Polyhedral
Base size	10 mm
Surface growth rate	Default
Target surface size	6 mm
Minimum surface size	1 mm
Number of prism layers	3
Prism layer stretching	1.25
Prism layer total thickness	5 mm
Volume growth rate	1.2
Maximum Tet size	15 mm

The polyhedral mesh type with a prism layer has been chosen due to its suitability for generating complex mesh models, its efficiency in construction, and its provision of fewer mesh cells compared to other mesh types. Additionally, the prism layer enhances the accuracy of the simulation. Figure 6 presents the polyhedral mesh type with a prism layer applied to the inner wall of the pipe. Mesh optimization has also been performed near the nozzle to further enhance the accuracy of the CFD flow analysis at the nozzle outlet.

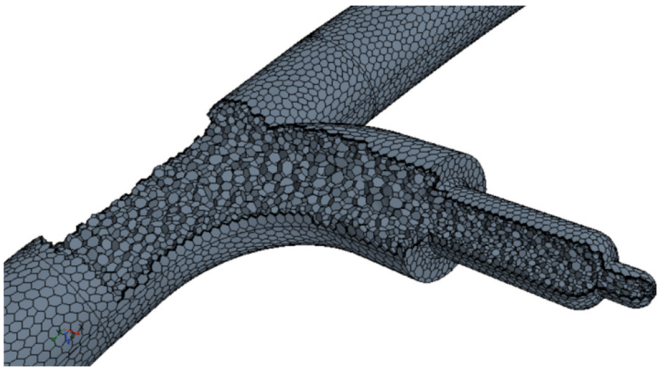

Fig. 6. Polyhedral density mesh near nozzle.

The boundary conditions have been established to define the parameters utilized in the CFD simulation. These parameters for the fluid domain are detailed in Table II, which outlines the variables for the desired viscous model.

TABLE II. DOMAIN PARAMETERS

Parameter	Values
Turbulence model	SST K-omega
Space	3D
Time	Steady
Fluid	Water at 70 °C
Density	977 kg/ m³
Gravity	9.807 m/s²
Inlet velocity	2 m/s, 3 m/s, 4 m/s, 5 m/s, 6 m/s, 7 m/s
Outlet	Pressure outlet

The SST K-omega turbulent model has been selected, as it provides more accurate calculations in both the near-wall region and the overall flow field. The water temperature was set at 70 °C to enhance the cleaning performance of the tank when using hot water. The key variables to be investigated include the inlet velocity, and the study aims to analyze the pressure distribution across each nozzle. Achieving a minimal pressure variation among the nozzles is crucial for ensuring an optimal pressure distribution throughout the system, which contributes to effective cleaning performance.

III. RESULTS AND DISCUSSION

The CFD analysis focuses on eight-pipe ring models with a residual target value below 0.001. A total of 2000 iterations was conducted by averaging the results across each ring model. The simulation outcomes include scalar pressure and vector velocity data. A plane was established in the XY coordinate system, and point probes—totaling eight—were strategically positioned at each nozzle to analyze the fluid parameters. Figure 7 illustrates the locations of these point probes on the nozzles, which capture the corresponding pressure and velocity values.

A. Determination of Optimum Inlet Velocity

This study aims to identify the optimal cleaning process for tank surfaces. To achieve this, it is essential to maintain the integrity of the nozzle in its optimal condition. The variations in nozzle pressure correspond to the water pressure impacting the tank's surface and may play a significant role in the effectiveness of the cleaning process. This simulation involved comparing pressure data at each nozzle outlet with an operating pressure of 3 bar. The hexagonal closed-loop with a Tee (Ha) ring model was employed in this experiment. Table III presents the results of the simulation data, detailing the inlet velocities used for each ring model.

TABLE III. SIMULATION RESULTS OF THE HEXAGONAL CLOSED-LOOP MODEL WITH A TEE (HA) RING UNDER VARYING INLET VELOCITY CONDITIONS

Inlet velocity (m/s)	Inlet pressure (bar)	Nozzle 1 (bar)	Nozzle 2 (bar)	Nozzle 3 (bar)	Nozzle 4 (bar)	Nozzle 5 (bar)	Nozzle 6 (bar)	Nozzle 7 (bar)	Nozzle 8 (bar)
2	0.4520	0.2315	0.2580	0.2252	0.2555	0.2584	0.2525	0.2586	0.2640
3	1.0154	0.5178	0.5777	0.5044	0.5720	0.5801	0.5666	0.5794	0.5920
4	1.7948	0.9129	1.0197	0.8902	1.0104	1.0218	1.0007	1.0238	1.0462
5	2.8183	1.4308	1.6000	1.3969	1.5943	1.6071	1.5701	1.6074	1.6432
6	4.0682	2.4620	2.3088	2.0155	2.2991	2.3193	2.2649	2.3200	2.3731
7	5.5368	3.3499	3.1418	2.7426	3.1263	3.1441	3.0760	3.1586	3.2268

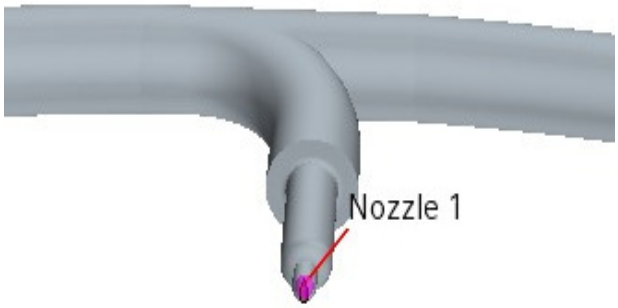

Fig. 7. Point probe location near nozzle.

The simulation results indicate that an increase in inlet velocity directly correlates with an increase in inlet pressure. Specifically, the simulations reveal that an inlet velocity of 7 m/s yields an average pressure of 3 bar at each nozzle outlet, which aligns with the findings of this study.

B. Pressure Distribution for Each Piping Ring Model

The simulation results from eight-ring models of scalar pressure were used to determine the fluid pressure at each nozzle outlet of the tank cleaning ring.

Figure 9 displays the pressure distribution at Nozzles 1 and 8. In both cases, the pressure near the nozzle outlet decreases due to the increase in velocity at the outlet. Nevertheless, the pressure at the nozzle remains at the desired level of 3 bar. Figure 9 also indicates that the branch region of the regular Tee pipe experiences a slight pressure increase relative to both the

upstream and downstream sections. In contrast, this phenomenon is not observed in the Y-type Tee, as shown in Figure 10, suggesting that the Y-type Tee promotes a more uniform pressure distribution compared to the conventional Tee configuration. A similar trend is observed in Figure 12, further validating the occurrence of this behavior in the regular Tee type.

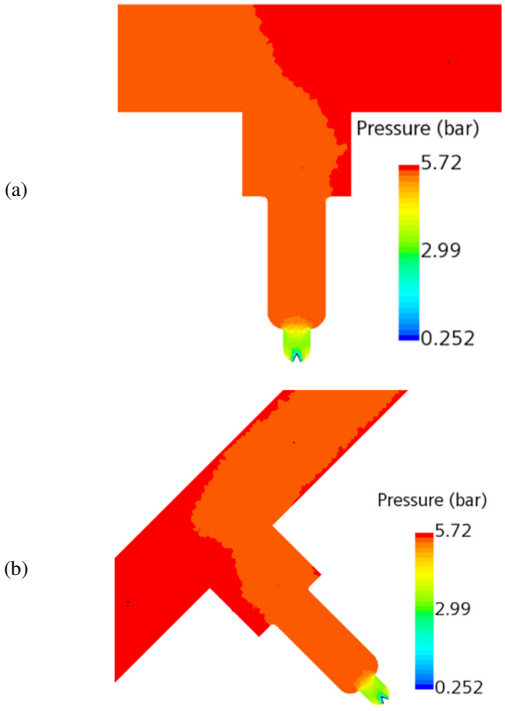

Fig. 8. Scalar pressure on hexagonal closed-loop model with a Tee (Ha): (a) Nozzle 1, (b) Nozzle 8.

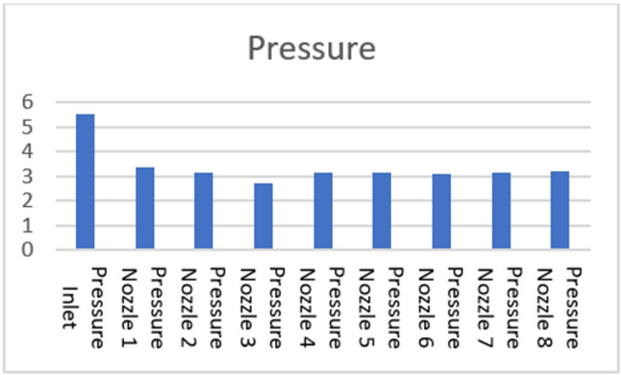

Fig. 9. Pressure distribution in hexagonal closed-loop model with a Tee (Ha).

The pressure distribution results presented in Figures 9, 11, and 13 reveal that the outlet nozzle pressures exhibit slight non-uniformity. In the hexagonal piping configuration of Figures 9 and 10, a more significant variation in pressure drop is observed among the nozzle outlets. In contrast, the circular ring configuration in Figure 13 demonstrates a more uniform pressure distribution across all outlets.

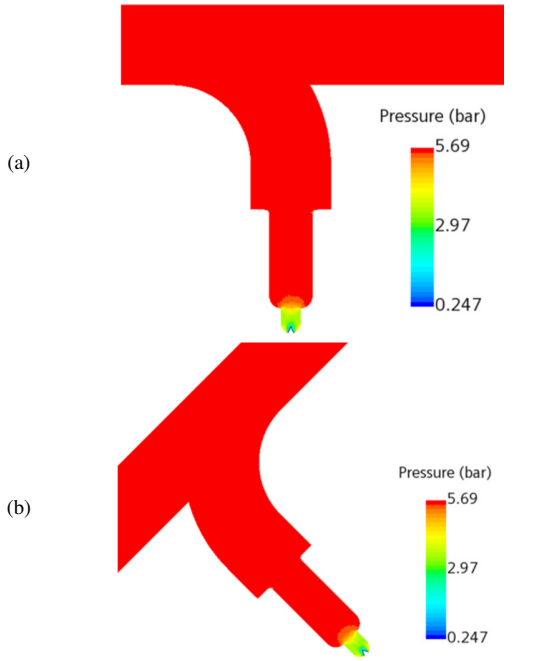

Fig. 10. Scalar pressure on hexagonal split open loop with Tee Y (Hc): (a) Nozzle 1, (b) Nozzle 8.

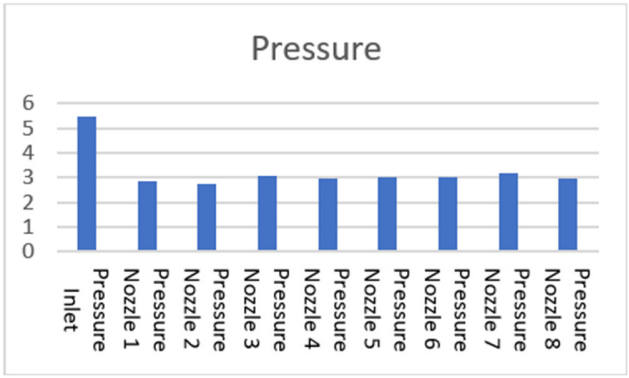

Fig. 11. Pressure distribution on a hexagonal split-open loop with Tee Y (Hc).

Additionally, Figures 8, 10, and 12 show the pressure build-up at the nozzle tips, which is consistent with the Bernoulli principle. The optimization analysis primarily focuses on the data presented in Figures 9, 11, and 13. The simulation results indicate that, in the circular closed-loop with the Tee (Ca) ring model, the difference between the minimum and the maximum pressure is approximately 10%, as outlined in Table IV. This represents the smallest pressure variation among all simulated ring models. Such a small variation ensures that the spray from each nozzle remains nearly uniform, thereby providing consistent cleaning coverage across the tank walls.

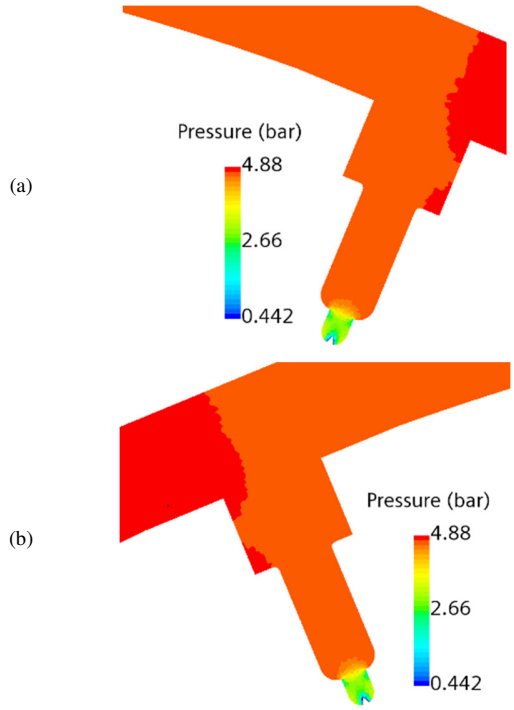

Fig. 12. Scalar pressure in circular closed-loop model with Tee (Ca): (a) Nozzle 1, (b) Nozzle 8.

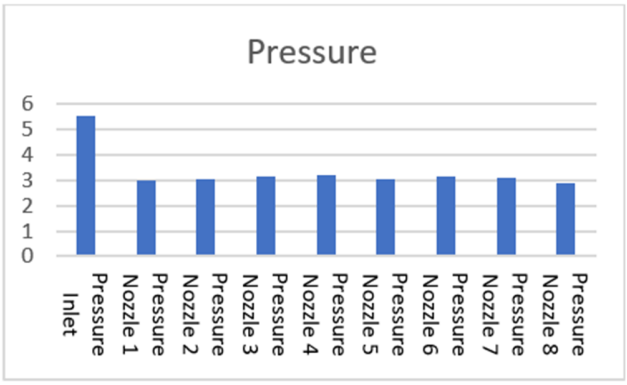

Fig. 13. Pressure distribution in circular closed-loop model with Tee (Ca).

C. Velocity Distribution on Each Ring Model

In addition to pressure, the fluid flow velocity within the tank cleaning ring is a vital parameter for analyzing the velocity pattern. Consequently, during the simulations, a velocity vector was generated to gain a better understanding of the fluid flow velocity pattern in the tank cleaning ring. The images in Figures 14, 16, and 18, along with Tables III-V, present the simulation results for each ring model conducted.

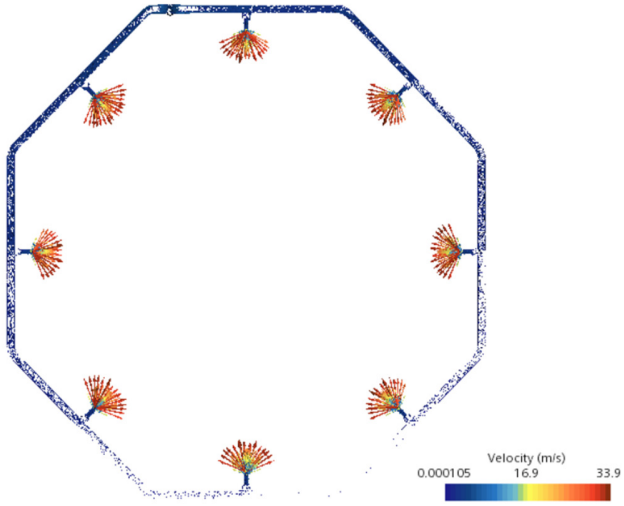

Fig. 14. Vector velocity on hexagonal closed-loop model with a Tee (Ha).

Figures 14, 16, and 18 present the velocity vector fields inside the piping system, along with the spraying direction at the nozzle outlets. The vector plots illustrate the flow behavior within the pipe network, highlighting the acceleration of fluid as it exits through the nozzle tips. This visualization provides insights into the distribution of momentum and the flow orientation, which are crucial in determining the overall effectiveness of the spray system.

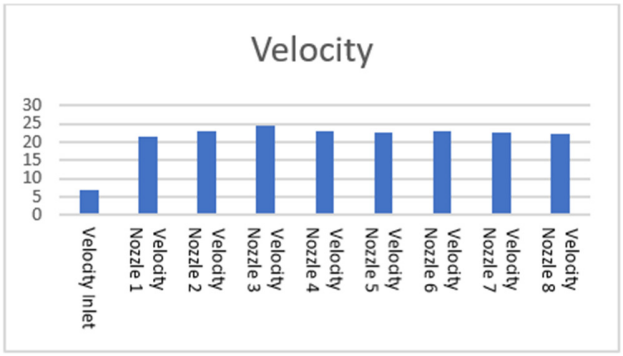

Fig. 15. Velocity distribution on hexagonal closed-loop model with a Tee (Ha).

TABLE IV. PRESSURE DISTRIBUTION IN PIPE RING MODELS

Ring models	Inlet pressure (bar)	Nozzle 1 (bar)	Nozzle 2 (bar)	Nozzle 3 (bar)	Nozzle 4 (bar)	Nozzle 5 (bar)	Nozzle 6 (bar)	Nozzle 7 (bar)	Nozzle 8 (bar)
Ha	5.5368	3.3499	3.1418	2.7425	3.1263	3.1440	3.0760	3.1586	3.2268
Hb	5.7387	3.1688	3.0007	2.7513	2.7956	2.9531	2.7829	3.1660	3.1199
Hc	5.4667	2.8575	2.7451	3.0774	2.9641	2.9925	3.0198	3.1630	2.9300
Hd	5.4499	2.9444	3.0879	3.0656	3.1752	2.9733	2.9796	3.0631	2.7476
Ca	5.5115	2.9778	3.0359	3.1265	3.2044	3.0474	3.1489	3.1044	2.8940
Cb	7.0249	4.4546	4.3163	4.6981	4.3194	4.4350	4.2130	4.7325	4.4928
Cc	5.4113	3.0025	3.1377	3.0853	3.0198	2.9831	2.6856	3.1365	3.0655
Cd	5.6016	3.0035	3.1594	3.0879	2.8993	2.9558	2.6993	3.1008	3.1162

TABLE V. VELOCITY DISTRIBUTION FOR PIPE RING MODEL

Ring models	Nozzle 1 (bar)	Nozzle 2 (bar)	Nozzle 3 (bar)	Nozzle 4 (bar)	Nozzle 5 (bar)	Nozzle 6 (bar)	Nozzle 7 (bar)	Nozzle 8 (bar)
Ha	21.6203	22.8707	24.4837	22.8927	22.4915	22.9886	22.5911	22.3846
Hb	22.6948	23.3934	24.2498	24.0964	23.4995	24.0050	22.5678	23.2994
Hc	24.1149	24.3814	23.1443	23.6730	23.3961	23.3685	22.5084	23.7882
Hd	23.4341	22.1134	23.3525	22.7024	23.4487	23.3629	23.0501	23.9108
Ca	23.3709	23.1866	22.7197	22.4974	23.2137	22.6154	22.8651	23.9007
Cb	21.1364	21.8865	20.2423	21.8203	21.9877	21.9190	22.4270	20.7732
Cc	22.9622	22.5035	22.9194	23.3201	23.3467	24.3934	22.5574	22.7503
Cd	23.1166	22.3990	22.7845	23.8514	23.5313	24.4200	22.9764	22.9870

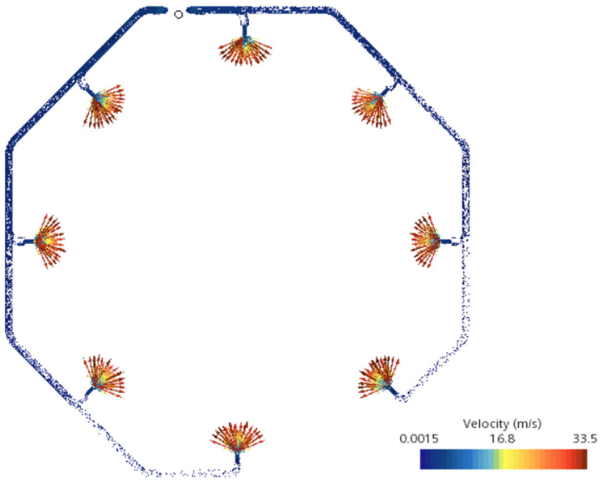

Fig. 16. Vector velocity on hexagonal split open-loop with Tee Y (Hc).

Tables III-V summarize the velocity distribution obtained from the simulations. In the circular closed-loop with the Tee (Ca) ring model, the difference between the minimum and maximum outlet velocities is approximately 6%. This represents the smallest velocity variation among all the ring configurations analyzed. A reduced velocity discrepancy across the nozzles is a key indicator of uniform flow distribution, ensuring that each nozzle delivers fluid at nearly the same momentum. This uniformity minimizes the local variations that could otherwise lead to an uneven spray coverage.

From a practical perspective, the near-uniform velocity distribution observed in the circular closed-loop with the Tee ring model carries significant implications for the cleaning efficiency. When the velocity differences among the nozzles are minimal, the resulting sprays are nearly identical in both strength and direction. This ensures that each nozzle dispenses a comparable volume of cleaning solution, providing consistent coverage across all tank walls. Such uniformity is essential in industrial cleaning applications as it not only enhances the fluid usage efficiency but also ensures reliability in meeting hygiene standards, helping to prevent untreated or under-cleaned areas within the tank.

D. Velocity Vector Distribution Comparison on Tee Components with Tee Y

Based on the design comparison simulation results, specific phenomena were observed in the cleaning ring. The findings demonstrate the utility of these simulations in selecting the Tee and Tee Y components within the circular closed-loop models: the Tee (Ca) ring model and the Tee Y (Cd) ring model, both of which feature a circular fundamental design. Table VI presents the fluid flow vector results for the Tee and Tee Y components.

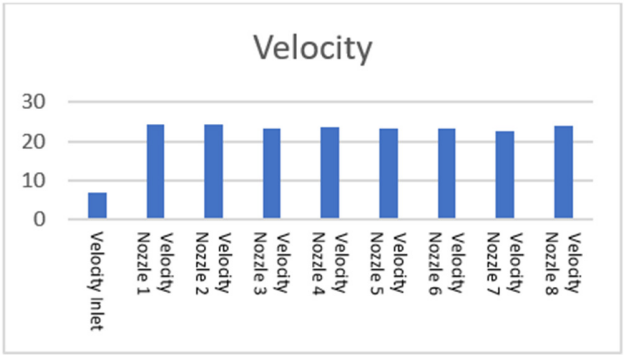

Fig. 17. Velocity distribution on hexagonal split open-loop with Tee Y (Hc).

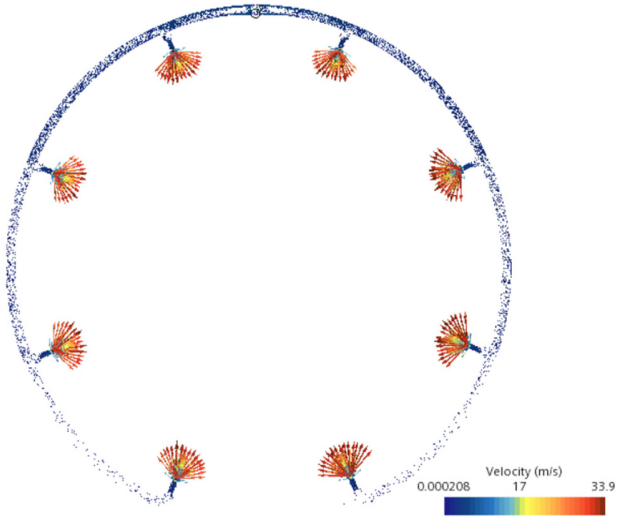

Fig. 18. Vector velocity in circular closed-loop model with Tee (Ca).

A notable distinction between the regular Tee and the Y-type Tee can be observed in the simulation results shown in Table VI. The Y-type Tee demonstrates significantly less swirling flow compared to the conventional Tee configuration. The presence of the swirling flow in the branch region is

undesirable, as it prolongs the residence time of the fluid within the branch. Increased residence time can adversely affect the flow stability, leading to non-uniform pressure and uneven flow distribution at the nozzle outlets. Consequently, the diminished swirling observed in the Y-type Tee promotes more efficient fluid transport and enhances the uniformity of the spray distribution, making it a preferred choice for applications that require consistent nozzle performance. Additionally, when simulating the ring model using a basic circular design, it was found that the incorporation of the Tee Y component resulted in improved velocity. This enhancement can be attributed to the positioning of the vortex in the Tee Y, which is located to the side, allowing the fluid flow to proceed uninterrupted. In contrast, a Tee with a vortex centered within the component would hinder the fluid flow toward the nozzle outlet.

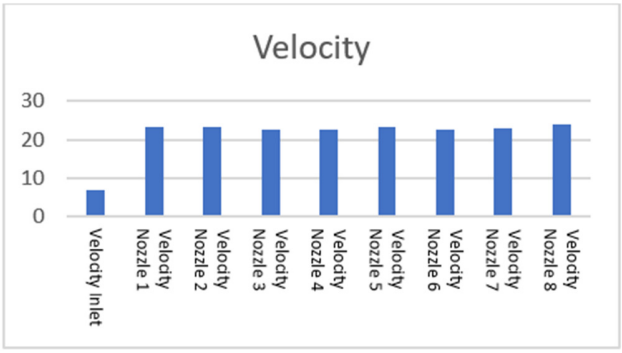

Fig. 19. Velocity distribution in circular closed-loop model with Tee (Ca).

TABLE VI. FLUID FLOW IN TEE AND TEE Y COMPONENTS

Circular Close-Loop Model with Tee (Ca)	**Circular Closed-Loop Model with Tee Y (Cd)**
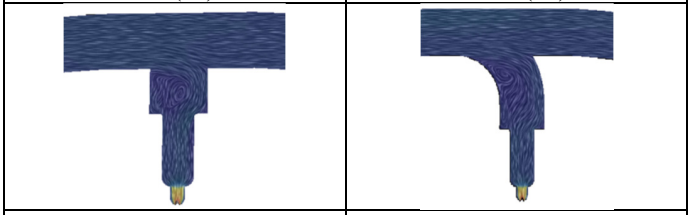	
Nozzle 1	Nozzle 1
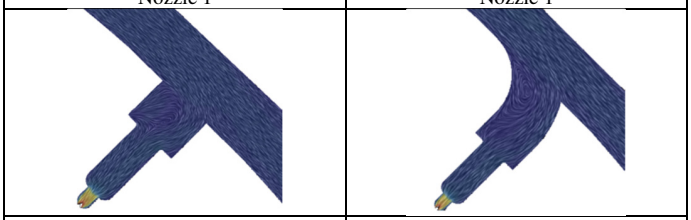	
Nozzle 2	Nozzle 2
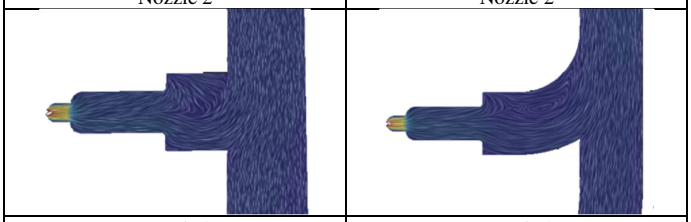	
Nozzle 3	Nozzle 3

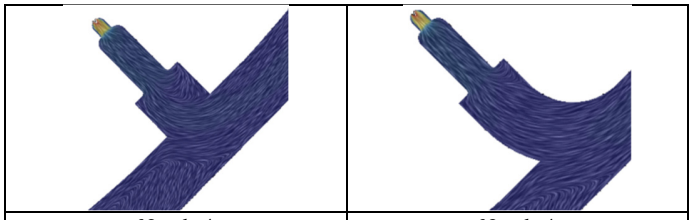	
Nozzle 4	Nozzle 4
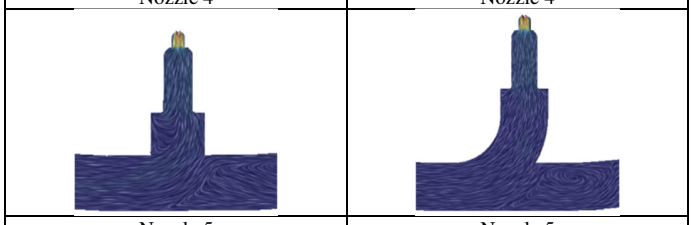	
Nozzle 5	Nozzle 5
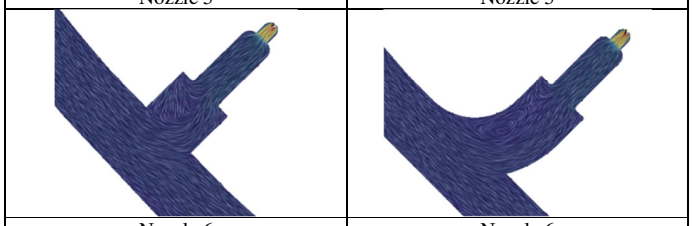	
Nozzle 6	Nozzle 6
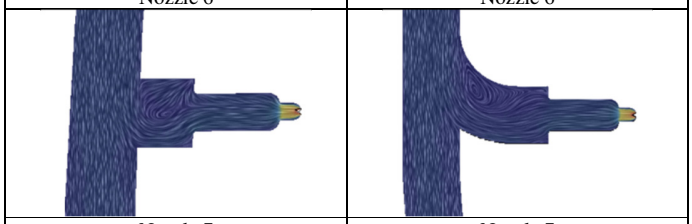	
Nozzle 7	Nozzle 7
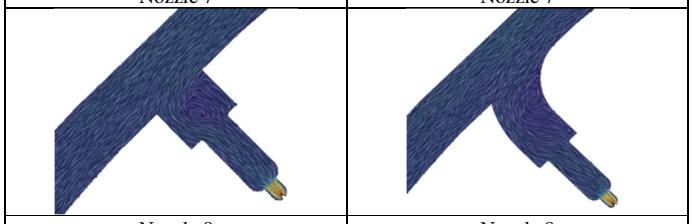	
Nozzle 8	Nozzle 8

E. Volume of Fluid Method (VoF)

The VoF method is a CFD simulation technique employed to model and understand the directional movement between two or more immiscible fluids. In the simulation conducted in this research, the VoF method proves to be highly valuable for multiphase modeling [11]. This method is beneficial when dealing with scenarios where two or more fluids coexist within the same conditions and space. This study makes it especially relevant when simulating the water discharge through the outlet nozzle, impacting the tank.

The VoF model is used for solving immiscible fluid problems. In this scenario, the implicit unsteady flow is chosen. The phase interaction is VoF–VoF phase with constant density, where the primary phase is air and the secondary phase is water. The model computes the spatial distribution of each phase using a transport equation for the phase volume fraction.

Accurate interface resolution can be achieved through higher-order discretization schemes and interface-capturing techniques, such as the High-Resolution Interface Capturing (HRIC) method. The computational efficiency is further enhanced by multi-stepping, which applies temporal sub-cycling to the volume fraction transport, thereby removing the limitations on the Courant number and improving the free-surface resolution.

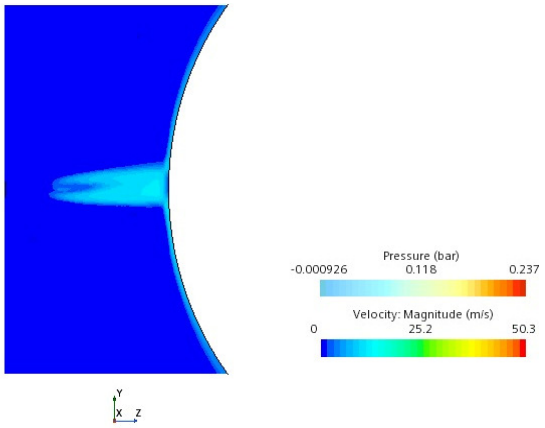

Fig. 20. Top view of the simulation results on the nozzle using the VoF method.

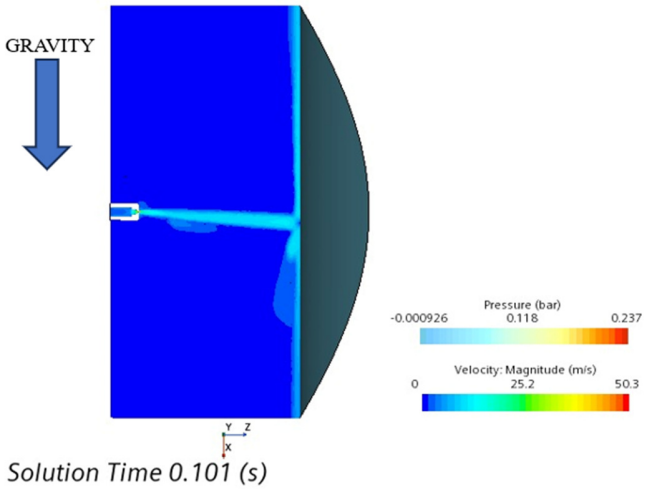

Fig. 21. Side view of the simulation results on the nozzle using the VoF method.

Figures 20 and 21 present the simulation results using the VoF method on Nozzle 8 of the circular closed-loop with the Tee (Ca) ring model. In the top view, as portrayed in Figure 20, water can be sprayed toward the tank, forming a fan shape; this is consistent with the flat fan nozzle characteristic. In the side view, as displayed in Figure 21, the simulation shows that the water flow, influenced by gravity, tends to move downward. The observation results, as shown in Figure 22, indicate that the effect of the water pressure on the nozzle area is relatively small, with a maximum pressure of 0.237 bar occurring on the tank surface.

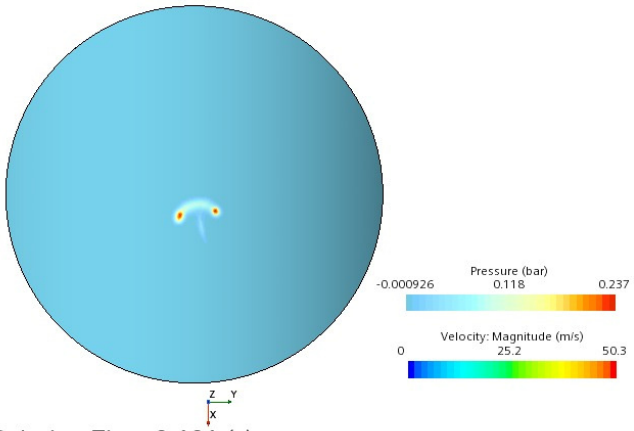

Fig. 22. Impact of water pressure on the tank.

F. Fluid Piping Installation Design Calculations

The research involves performing calculations to select the appropriate pump specifications. This was done/achieved by considering the cross-sectional area of the pipe and the head loss that occurs in the fluid while it flows through the pipe. After carrying out the calculations, the result of the fluid discharge required in the tank cleaning machine installation is 0.00266 m³/s, and the Reynolds number is 372.420,79. Re > 4.000 indicates turbulent flow. Figure 23 depicts the piping system diagram, which is used as a reference for the calculation of head loss. The piping considerations are calculated in the discharge section to the pipe ring connection.

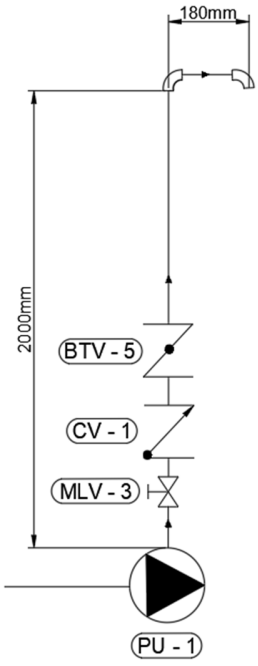

Fig. 23. Pipe system schematic configuration.

$$f = \frac{2\Delta PD}{\rho LV^2} \quad (1)$$

$$f = \frac{8 \times 1.171\ Pa}{\frac{977kg}{m^3} \times (7\ m/s)^2} = 0.000196$$

$$h_f = f\frac{Lv_1{}^2}{D2g} \quad (2)$$

$$H_{LMayor} = 0.000196 \frac{2.18m\ (7\ m/s)^2}{0.022m \times 2 \times 9.81 m/s^2}$$

$$H_{LMayor} = 0.485\text{m} \quad (3)$$

TABLE VII. PIPE LOSS COEFFICIENT

Component name	Number	Loss coefficient
Sanitary elbow 90°	2	0.131
Manual valve	1	0.15
Check valve	1	1.20
Solenoid valve	1	0.15

$$H_{LMinor} = K_{total}\frac{v^2}{2g} \quad (4)$$

$$H_{LMinor} = 1.762 \frac{7\ m/s^2}{2x9.81 m/s^2} \quad (5)$$

$$H_{LMinor} = 0.628\ m$$

In the installation of the tank cleaning machine, a plastic hose with a roughness value of 0 (indicating smoothness) is employed. As a result, the significant head losses within the hose can be disregarded, given that the curved hose's head loss is minimal, measuring only 0.066 m. The simulation indicates an average inlet pressure of 5.5 bar at the tank cleaning ring. This analysis calculates the head loss occurring at the inlet pressure ring of the tank cleaning ring, which amounts to 57.442 m. The total head loss can be calculated by summing all the losses in the discharge pipe system:

$$H_{L\,Total}\,Installation = 0.485\ m + 0.628\ m\ + 0\ m + 0.066\ m + 57.442$$

$$H_{L\,Total}\,Installation = 58.621\ m$$

Therefore, the total head loss for this piping installation from the pump to the inlet piping ring is 58.621m.

IV. CONCLUSION

This study demonstrated the effectiveness of Computational Fluid Dynamics (CFD) in examining piping installation ring models. The circular closed-loop with Tee (Ca) configuration exhibited superior hydraulic performance compared to the hexagonal design, achieving a pressure distribution variation of 10% and a velocity variation of 6%, ensuring more uniform spray delivery.

The Y-type Tee further improved the system performance by reducing the vortex formation and enhancing the flow alignment, whereas the regular Tee induced swirling that led to non-uniform distribution. For the proposed system using a 1-inch diameter pipe, the required pump specification was 0.00266 m³/s discharge and 58.621 m head. The Volume of Fluid Method (VoF) confirmed that at a spraying distance of 20 cm, the impact pressure was 0.237 bar, sufficient for effective cleaning.

These findings highlight that adopting a circular closed-loop configuration with Y-type Tee fittings improves the flow uniformity, energy efficiency, and spray consistency, making it preferable for industrial tank-cleaning applications.

ACKNOWLEDGMENT

The authors extend their heartfelt gratitude to Universitas Tarumanagara and INTI International University for their invaluable support throughout this research. Their encouragement and resources have made a significant impact on this work.

REFERENCES

[1] A. Svoboda, M. Chalupa, and J. Jelínek, "Modern Technical Solutions for Cleaning, Disinfection and Sterilization," *Manufacturing Technology*, vol. 22, no. 6, pp. 754–763, Jan. 2023, https://doi.org/10.21062/mft.2022.089.

[2] J. M. Wilson and S. K. Venayagamoorthy, "Evaluation of Hydraulic Efficiency of Disinfection Systems Based on Residence Time Distribution Curves," *Environmental Science & Technology*, vol. 44, no. 24, pp. 9377–9382, Dec. 2010, https://doi.org/10.1021/es102861g.

[3] W. Karamti, S. El Khediri, and T. Moulahi, "Sustainable Wastewater Management in Agriculture: A Deep Learning-based Olive Classification for Resource Efficiency in Water-Scarce Regions," *Engineering, Technology & Applied Science Research*, vol. 15, no. 3, pp. 24061–24069, June 2025, https://doi.org/10.48084/etasr.10667.

[4] S. W. Hung and J.-K. Kim, "Optimization of Water Systems with the Consideration of Pressure Drop and Pumping," *Industrial & Engineering Chemistry Research*, vol. 51, no. 2, pp. 848–859, Jan. 2012, https://doi.org/10.1021/ie201775y.

[5] M. H. H. Ishak *et al.*, "Numerical Analysis of Nozzle Flow and Spray Characteristics from Different Nozzles Using Diesel and Biofuel Blends," *Energies*, vol. 12, no. 2, Jan. 2019, Art. no. 281, https://doi.org/10.3390/en12020281.

[6] F. A. Hamad *et al.*, "Investigation of Pressure Drop in Horizontal Pipes with Different Diameters," *International Journal of Multiphase Flow*, vol. 91, pp. 120–129, May 2017, https://doi.org/10.1016/j.ijmultiphaseflow.2017.01.007.

[7] U. Hayyat *et al.*, "CFD Simulation of a Forced Draft Biomass Cookstove for Different Airflow Conditions," *Results in Engineering*, vol. 21, Mar. 2024, Art. no. 101928, https://doi.org/10.1016/j.rineng.2024.101928.

[8] S. Darmawan and H. Tanujaya, "CFD Investigation of Flow Over a Backward-facing Step using an RNG k-? Turbulence Model," *International Journal of Technology*, vol. 10, no. 2, Apr. 2019, Art. no. 280, https://doi.org/10.14716/ijtech.v10i2.800.

[9] M. Sularso and H. Tahara, *Pumps and Compressors, Selection, Use and Maintenance*, 9th ed. Jalan Bunga, Jakarta, Indonesia: PT Pradnya Paramita., 2006.

[10] Y. Triafandy, A. B. Pulungan, and H. Hamdani, "Kendali Solar Tracker Menggunakan Selenoid Valve Sebagai Pengendali Aliran fluida," *JTEIN: Jurnal Teknik Elektro Indonesia*, vol. 1, no. 2, pp. 174–178, Nov. 2020, https://doi.org/10.24036/jtein.v1i2.66.

[11] X. Wang *et al.*, "Effect of Injection Pressure on Low-temperature Fuel Atomization Characteristics of Diesel Engines Under Cold Start Conditions," *International Journal of Multiphase Flow*, vol. 172, Feb. 2024, Art. no. 104712, https://doi.org/10.1016/j.ijmultiphaseflow.2023.104712.